11018 *Inorg. Chem.* **2010**, *49*, 11018–11029
DOI: 10.1021/ic101574a

Inorganic Chemistry
Article

Dependence of the Chemical Properties of Macrocyclic $[Ni^{II}_2L(\mu\text{-}O_2CR)]^+$ Complexes on the Basicity of the Carboxylato Coligands (L^{2-} = macrocyclic N_6S_2 ligand)

Ulrike Lehmann,[†] Julia Klingele,[‡] Vasile Lozan,[†,§] Gunther Steinfeld,[‡] Marco H. Klingele,[‡] Steffen Käss,[†,∥] Axel Rodenstein,[†] and Berthold Kersting*[,†]

[†]*Institut für Anorganische Chemie, Universität Leipzig, Johannisallee 29, D-04103 Leipzig, Germany, and* [‡]*Institut für Anorganische und Analytische Chemie, Albert-Ludwigs-Universität Freiburg, Albertstr. 21, D-79104 Freiburg, Germany.* [§]*Present address: Laboratory of Coordination Chemistry, Institute of Chemistry, Academy of Sciences of Moldova, Academiei str. 3, MD-2028 Chisinau, Republic of Moldova.* [∥]*Present address: Avancis GmbH & Co. KG, D-04860 Torgau, Germany*

Received August 4, 2010

The dependence of the properties of mixed ligand $[Ni^{II}_2L(\mu\text{-}O_2CR)]^+$ complexes (where L^{2-} represents a 24-membered macrocyclic hexaamine-dithiophenolato ligand) on the basicity of the carboxylato coligands has been examined. For this purpose 19 different $[Ni^{II}_2L(\mu\text{-}O_2CR)]^+$ complexes (**2**−**20**) incorporating carboxylates with pK_b values in the range 9 to 14 have been prepared by the reaction of $[Ni^{II}_2L(\mu\text{-}Cl)]^+$ (**1**) and the respective sodium or triethylammonium carboxylates. The resulting carboxylato complexes, isolated as ClO_4^- or BPh_4^- salts, have been fully characterized by elemental analyses, IR, UV/vis spectroscopy, and X-ray crystallography. The possibility of accessing the $[Ni^{II}_2L(\mu\text{-}O_2CR)]^+$ complexes by carboxylate exchange reactions has also been examined. The main findings are as follows: (*i*) Substitution reactions between **1** and NaO_2CR are not affected by the basicity or the steric hindrance of the carboxylate. (*ii*) Complexes **2**−**20** form an isostructural series of bisoctahedral $[Ni^{II}_2L(\mu\text{-}O_2CR)]^+$ compounds with a $N_3Ni(\mu\text{-}SR)_2(\mu\text{-}O_2CR)NiN_3$ core. (*iii*) They are readily identified by their ν_{as}(CO) and ν_s(CO) stretching vibration bands in the ranges 1684−1576 cm^{-1} and 1428−1348 cm^{-1}, respectively. (*iv*) The spin-allowed $^3A_{2g} \rightarrow {}^3T_{2g}$ (ν_1) transition of the $NiOS_2N_3$ chromophore is steadily red-shifted by about 7.5 nm per pK_b unit with increasing pK_b of the carboxylate ion. (*v*) The less basic the carboxylate ion, the more stable the complex. The stability difference across the series, estimated from the difference of the individual ligand field stabilization energies (LFSE), amounts to about 4.2 kJ/mol [Δ_{LFSE}(**2**,**18**)]. (*vi*) The "second-sphere stabilization" of the nickel complexes is not reflected in the electronic absorption spectra, as these forces are aligned perpendicularly to the Ni−O bonds. (*vii*) Coordination of a basic carboxylate donor to the $[Ni^{II}_2L]^{2+}$ fragment weakens its Ni−N and Ni−S bonds. This bond weakening is reflected in small but significant bond length changes. (*viii*) The $[Ni^{II}_2L(\mu\text{-}O_2CR)]^+$ complexes are relatively inert to carboxylate exchange reactions, except for the formato complex $[Ni^{II}_2L(\mu\text{-}O_2CH)]^+$ (**8**), which reacts with both more and less basic carboxylato ligands.

Introduction

Dinucleating Robson-type amino-thiophenolato ligands have received considerable attention over the past several decades,[1−3] especially as supporting ligands for the preparation of model compounds for dinuclear metalloenzymes,[4] for the stabilization of unusual metal oxidation states,[5] and to understand, achieve, and control dinuclear metal reactivity.[6,7]

*To whom correspondence should be addressed. E-mail: b.kersting@uni-leipzig.de.

(1) Pilkington, N. H.; Robson, R. *Aust. J. Chem.* **1970**, *23*, 2225–2236.
(2) (a) Atkins, A. J.; Blake, A. J.; Schröder, M. *J. Chem. Soc., Chem. Commun.* **1993**, 1662–1665. (b) Branscombe, N. D. J.; Blake, A. J.; Marin-Becerra, A.; Li, W.-S.; Parsons, S.; Ruiz-Ramirez, L.; Schröder, M. *J. Chem. Soc., Chem. Commun.* **1996**, 2573–2574.
(3) (a) Brooker, S.; Croucher, P. D. *J. Chem. Soc., Chem. Commun.* **1995**, 1493–1494. (b) Brooker, S.; Croucher, P. D. *J. Chem. Soc., Chem. Commun.* **1995**, 2075–2076. (c) Brooker, S.; Croucher, P. D.; Roxburgh, F. M. *J. Chem. Soc., Dalton Trans.* **1996**, 3031–3037. (d) Brooker, S.; Croucher, P. D. *J. Chem. Soc., Chem. Commun.* **1997**, 459–460.
(4) Atkins, A. J.; Black, D.; Blake, A. J.; Marin-Becerra, A.; Parsons, S.; Ruiz-Ramirez, L.; Schröder, M. *J. Chem. Soc., Chem. Commun.* **1996**, 457–464.
(5) (a) Brooker, S.; Croucher, P. D.; Davidson, T. C.; Dunbar, G. S.; McQuillan, A. J.; Jameson, G. B. *J. Chem. Soc., Chem. Commun.* **1998**, 2131–2132. (b) Spencer, D. J. E.; Marr, A. C.; Schröder, M. *Coord. Chem. Rev.* **2001**, *219*−*221*, 1055–1074.
(6) Gavrilova, A. L.; Jin Qin, C.; Sommer, R. D.; Rheingold, A. L.; Bosnich, B. *J. Am. Chem. Soc.* **2002**, *124*, 1714–1722.
(7) (a) Brooker, S. *Coord. Chem. Rev.* **2001**, *222*, 33–56. (b) Brooker, S.; Croucher, P. D.; Davidson, T. C.; Dunbar, G. S.; Beck, C. U.; Subramanian, S. *Eur. J. Inorg. Chem.* **2000**, 169–179.

 Published on Web 11/10/2010 © 2010 American Chemical Society

Chart 1

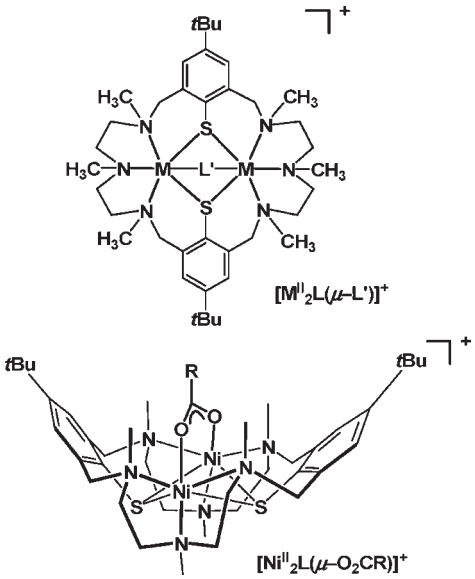

We are interested in the coordination chemistry of the octadentate amino-thiophenolato ligand L^{2-} (Chart 1), which supports mixed-ligand $[M^{II}{}_2L(\mu\text{-}L')]^+$ complexes (L′ = coligand) with a doubly thiolato-bridged $N_3M(\mu\text{-}SR)_2(\mu\text{-}L')MN_3$ core structure.[8,9]

Several sets of closely related $[M^{II}{}_2L(\mu\text{-}L')]^+$ complexes have now been prepared, and their stability,[10] reactivity,[11,12] and electronic structure[13,14] have been studied as a function of the type of coligand (or the *d* electron configuration of the metal ion). One series comprises dinuclear $[Ni^{II}{}_2L(\mu\text{-}L')]^+$ complexes bearing different coligands (e.g., L′ = Cl^-, OH^-,[15] SH^-,[10] NO_2^-, NO_3^-, N_3^-, N_2H_4,[16] $CH_3CO_2^-$, HCO_3^-, $H_2PO_4^-$,[17] ClO_4^-, ReO_4^-, CrO_4^{2-}, MoO_4^{2-}, WO_4^{2-},[18] alkyl carbonates ($ROCO_2^-$),[19] alkyl carbamates ($RNCO_2^-$),[20] pyrazolate, tetrazolate,[21] and tetrahydridoborate (BH_4^-)[22]). In another set of complexes the divalent metal ions vary while the coligand remains the same (e.g., $[M^{II}{}_2L(\mu\text{-}O_2CCH_3)]^+$, M^{II} = Mn, Fe, Co, Ni, Zn,[23] Cd[24]). The third series comprises isostructural zinc(II) carboxylato complexes, $[Zn^{II}{}_2L(\mu\text{-}O_2CR)]^+$, differing only in the basicity of the carboxylato coligand.[17] From these studies, we became very familiar with the coordination chemistry of the amino-thiophenolato ligand L^{2-} and its various derivatives[25] and have been able to derive magneto-structural[9,26] and structure−reactivity relationships.[11,12]

As part of this program, we sought to extend our exploration to the syntheses of dinuclear nickel(II) complexes incorporating carboxylato coligands of different basicity. Our motivation was based on the following reasons: (*i*) Carboxylato ligands are of general importance in coordination chemistry.[27] (*ii*) Carboxylate ions are biologically relevant molecules.[28−33] (*iii*) Nickel carboxylate bonding is of importance in bioinorganic[34,35] and biomimetic chemistry.[36,37] (*iv*) A systematic study of an isostructural series of carboxylato-bridged nickel(II) complexes has not appeared in the literature.[38] (*v*) The characterization data of carboxylato-bridged $[Ni^{II}{}_2L(\mu\text{-}O_2CR)]^+$ complexes may serve as invaluable references for future studies aimed at regioselective carboxylate transformations.[12,39−41] (*vi*) Since the immediate environment of the carboxylate group in the dinuclear complexes is essentially the same, these systems should be well suited for the study of complex properties as a function of varying carboxylato coligand basicity.

In this study we describe the synthesis and spectroscopic properties of 19 bisoctahedral carboxylato complexes of the type $[Ni^{II}{}_2L(\mu\text{-}O_2CR)]^+$ incorporating carboxylates with pK_b values in the range 9−14. It was possible to determine the crystal structures of most of the complexes by single crystal X-ray diffraction, so that structural and spectroscopic

(8) Kersting, B. *Z. Anorg. Allg. Chem.* **2004**, *630*, 765–780.
(9) Lozan, V.; Loose, C.; Kortus, J.; Kersting, B. *Coord. Chem. Rev.* **2009**, *253*, 2244–2260.
(10) Lozan, V.; Kersting, B. *Inorg. Chem.* **2008**, *47*, 5386–5393.
(11) Kersting, B. In *Activating Unreactive Molecules - The Role of secondary Interactions*; Bolm, C., Hahn, F. E., Eds.; Wiley-VCH: Weinheim, 2009; Chapter 1, pp 1−17.
(12) Kersting, B.; Lehmann, U. Chemistry of Metalated Container Molecules. In *Advances in Inorganic Chemistry*; van Eldik, R., Hubbard, C. D., Eds.; Elsevier: Amsterdam, The Netherlands, 2009; Vol. *61*, pp 407−470.
(13) Chaudhuri, P.; Kataev, V.; Büchner, B.; Klauss, H.-H.; Kersting, B.; Meyer, F. *Coord. Chem. Rev.* **2009**, *253*, 2261–2285.
(14) Loose, C.; Ruiz, E.; Kersting, B.; Kortus, J. *Chem. Phys. Lett.* **2008**, *452*, 38–43.
(15) (a) Kersting, B.; Steinfeld, G. *Chem. Commun.* **2001**, 1376–1377. (b) Klingele, M. H.; Steinfeld, G.; Kersting, B. *Z. Naturforsch.* **2001**, *56b*, 901–907.
(16) Hausmann, J.; Klingele, M. H.; Lozan, V.; Steinfeld, G.; Siebert, D.; Journaux, Y.; Girerd, J.-J.; Kersting, B. *Chem.—Eur. J.* **2004**, *10*, 1716–1728.
(17) Kersting, B. *Angew. Chem.* **2001**, *113*, 4109–4112. Kersting, B. *Angew. Chem., Int. Ed.* **2001**, *40*, 3987–3990.
(18) Lozan, V.; Kersting, B. *Eur. J. Inorg. Chem.* **2007**, 1436–1443.
(19) Gressenbuch, M.; Lozan, V.; Steinfeld, G.; Kersting, B. *Eur. J. Inorg. Chem.* **2005**, 2223–2234.
(20) Lozan, V.; Holldorf, J.; Kersting, B. *Inorg. Chim. Acta* **2009**, *362*, 793–798.
(21) Lozan, V.; Voitekhovich, S. V.; Gaponik, P. N.; Ivashkevich, O. A.; Kersting, B. *Z. Naturforsch.* **2008**, *63b*, 496–502.
(22) Journaux, Y.; Lozan, V.; Hausmann, J.; Kersting, B. *Chem. Commun.* **2006**, 83–84.
(23) Journaux, Y.; Glaser, T.; Steinfeld, G.; Lozan, V.; Kersting, B. *J. Chem. Soc., Dalton Trans.* **2006**, 1738–1748.
(24) Lozan, V.; Kersting, B. *Eur. J. Inorg. Chem.* **2005**, 504–512.
(25) Gregor, T.; Weise, C. F.; Lozan, V.; Kersting, B. *Synthesis* **2007**, 3706–3712.
(26) Chaudhuri, P.; Kataev, V.; Büchner, B.; Klauss, H.-H.; Kersting, B.; Meyer, F. *Coord. Chem. Rev.* **2009**, *253*, 2261–2285.
(27) Cotton, F. A.; Wilkinson, G.; Murillo, C. A.; Bochmann, M. *Advanced Inorganic Chemistry*, 6th ed.; John Wiley & Sons: New York, 1999; pp 486−488.
(28) Lipscomb, W. N.; Sträter, N. *Chem. Rev.* **1996**, *96*, 2375–2433.
(29) Lee, D.; Hung, P. L.; Spingler, B.; Lippard, S. J. *Inorg. Chem.* **2002**, *41*, 521–531.
(30) Lippard, S. J.; Berg, J. M. *Principles of Bioinorganic Chemistry*; University Science Books: Mill Valley, CA, 1994.
(31) Tshuva, E. Y.; Lippard, S. *J. Chem. Rev.* **2004**, *104*, 987–1012.
(32) Tolman, W. B.; Que, L., Jr. *J. Chem. Soc., Dalton Trans.* **2002** 653–660.
(33) Que, L.; Dong, Y. *Acc. Chem. Res.* **1996**, *29*, 190–196.
(34) Jabri, E.; Carr, M. B.; Hausinger, R. P.; Karplus, P. A. *Science* **1995**, *268*, 998–1004.
(35) Lippard, S. J. *Science* **1995**, *268*, 996–997.
(36) (a) Yamaguchi, K.; Koshino, S.; Akagi, F.; Suzuki, M.; Uehara, A.; Suzuki, S. *J. Am. Chem. Soc.* **1997**, *119*, 5752–5753. (b) Carlsson, H.; Haukka, M.; Bousseksou; Latour, J.-M.; Nordlander, E. M. *Inorg. Chem.* **2004**, *43*, 8252–8262.
(37) Harrop, T. C.; Mascharak, P. K. In *Concepts and Models in Bioinorganic Chemistry*; Kraatz, H.-B., Metzler-Nolte, N., Eds.; Wiley-VCH: Weinheim, Germany, 2006.
(38) Kumar, N.; Kachroo, P. L.; Kant., R. *Bull. Chem. Soc. Jpn.* **1980**, *53*, 1787–1788.
(39) Steinfeld, G.; Lozan, V.; Kersting, B. *Angew. Chem.* **2003**, *115*, 2363–2365. Steinfeld, G.; Lozan, V.; Kersting, B. *Angew. Chem., Int. Ed.* **2003**, *42*, 2261–2263.
(40) Käss, S.; Gregor, T.; Kersting, B. *Angew. Chem.* **2006**, *118*, 107–110. Käss, S.; Gregor, T.; Kersting, B. *Angew. Chem., Int. Ed.* **2006**, *45*, 101–104.
(41) Steinfeld, G.; Lozan, V.; Krüger, H.-J.; Kersting, B. *Angew. Chem.* **2009**, *121*, 1988–1991. Steinfeld, G.; Lozan, V.; Krüger, H.-J.; Kersting, B. *Angew. Chem., Int. Ed.* **2009**, *48*, 1954–1957.

information is now available for an isostructural series of $[Ni^{II}_2L(\mu\text{-}O_2CR)]^+$ compounds with carboxylate pK_b values differing by as much as five. The interplay of the basicities of the carboxylato coligands and the structural and spectroscopic features of the nickel(II) complexes are discussed.

Experimental Section

General Methods and Instrumentation. All manipulations were carried out under an argon atmosphere using standard Schlenk techniques. Reagent grade solvents were used throughout. Melting points were determined with a Waters Electrothermal 7200 instrument in open glass capillaries and are uncorrected. IR spectra were recorded on a Bruker TENSOR 27 FT-IR-spectrometer. Electronic absorption spectra were recorded on a JASCO V670 UV/vis/NIR spectrometer. Elemental analyses were carried out with a VARIO EL elemental analyzer.

Starting Materials. Complex $[Ni^{II}_2L(\mu\text{-}Cl)][ClO_4]$ (**1**[ClO_4]) was prepared according to the literature procedure.[15] All other reagents were obtained from standard commercial sources and used without further purifications. ***Caution!*** *Perchlorate salts of transition metal complexes are hazardous and may explode. Only small quantities should be prepared and great care taken.*

General Procedures for the Preparation of the Carboxylato-Bridged Nickel(II) Complexes 2−20. (a). $[Ni^{II}_2L(\mu\text{-}O_2CR)][ClO_4]$. To a solution of the chlorido-bridged complex **1**[ClO_4] (92 mg, 0.10 mmol) in MeOH (30 mL) was added a MeOH solution of the sodium or triethylammonium salt of the carboxylic acid (0.20 mmol) in MeOH (5 mL). The reaction mixture was stirred for 2 to 3 h during which time the color of the solution turned pale green. A solution of $LiClO_4 \cdot 3H_2O$ (0.80 g, 5.00 mmol) in MeOH (2 mL) was added. The resulting microcrystalline solid was isolated by filtration and dried in air. The crude product was dissolved in MeCN (30 mL) and filtered. EtOH (30 mL) was then added. The solution was concentrated by rotary evaporation (final volume ca. 10 mL) until incipient precipitation, and was then allowed to stand for another 6 h. The crude product was filtered, purified by recrystallization from a mixed MeCN/EtOH (1:1) solvent system, and dried in air.

(b). $[Ni^{II}_2L(\mu\text{-}O_2CR)][BPh_4]$. The tetraphenylborate salts were obtained as green powders by adding a solution of $NaBPh_4$ (342 mg, 1.00 mmol) in MeOH (3 mL) to a solution of $[Ni^{II}_2L(\mu\text{-}O_2CR)][ClO_4]$ (0.10 mmol) in MeOH (50−75 mL). The crude product was filtered, purified by recrystallization from a mixed MeCN/EtOH (1:1) solvent system, and dried in vacuo.

Characterization Data for the New Complexes. $[Ni^{II}_2L(\mu\text{-}O_2CCF_3)][ClO_4]$ (2[ClO_4]). Yield: 95 mg (95%); M.p.: 353−354 °C (decomp.); IR (KBr disk): [$\bar{\nu}$/cm^{-1} = 1684 s [$\nu_{as}(RCO_2^-)$], 1348 w [$\nu_s(RCO_2^-)$], 1208 s, 1144 s [ν(C−F)]; UV/vis (MeCN): λ_{max}/nm (ε/M^{-1} cm^{-1}) = 646 (36), 910sh, 1094 (73). Elemental analysis (%) calcd. for $C_{40}H_{64}ClF_3N_6Ni_2O_6S_2$ (998.94): C 48.09, H 6.46, N 8.41, S 6.42; found: C 47.93, H 6.35, N 8.32, S 6.61. **2**[BPh_4]: Yield: 121 mg (99%); M.p.: 299−301 °C (decomp.); Elemental analysis (%) calcd. for $C_{64}H_{84}BF_3N_6Ni_2O_2S_2$ (1218.71): C 63.07, H 6.95, N 6.90, S 5.26; found: C 62.85, H 6.83, N 6.87, S 5.39; IR (KBr disk): [$\bar{\nu}$/cm^{-1} = 1684 s [$\nu_{as}(RCO_2^-)$], 1349 w [$\nu_s(RCO_2^-)$], 1210 s, 1147 s [$\bar{\nu}$(C−F)]. This compound was additionally characterized by X-ray crystal structure analysis.

$[Ni^{II}_2L(\mu\text{-}O_2CCCl_3)][ClO_4]$ (3[ClO_4]). Yield: 89 mg (85%); M.p.: 318−320 °C (decomp.); IR (KBr disk): $\bar{\nu}$/cm^{-1} = 1683 s [$\nu_{as}(RCO_2^-)$], 1349 s [$\nu_s(RCO_2^-)$], 840 m, 746 m [ν(C−Cl)], 681 m [ν(C−Cl)]; UV/vis (MeCN): λ_{max}/nm (ε/M^{-1} cm^{-1}) = 649 (36), 907 sh, 1088 (77). **3**[BPh_4]: Yield: 121 mg (95%); Mp 230−232 °C (decomp.). Elemental analysis (%) calcd. for $C_{40}H_{64}Cl_4N_6Ni_2O_6S_2$ (1048.30): C 45.83, H 6.15, N 8.02, S 6.12; found: C 45.67, H 6.23, N 7.93, S 6.06. Elemental analysis (%) calcd. for $C_{64}H_{84}BCl_3N_6Ni_2O_2S_2$ (1268.08): C 60.62, H 6.68, N 6.63, S 5.06; found: C 60.46, H 6.93, N 6.65, S 4.94; IR (KBr disk): $\bar{\nu}$/cm^{-1} = 1682 s [$\nu_{as}(RCO_2^-)$], 1348 s [$\nu_s(RCO_2^-)$], 746 m [ν(C−Cl)], 680 m [ν(C−Cl)]; UV/vis (MeCN): λ_{max}/nm (ε/M^{-1} cm^{-1}) = 648 (45), 908 sh, 1087 (85). This compound was additionally characterized by X-ray crystal structure analysis.

$[Ni^{II}_2L(\mu\text{-}O_2CCHCl_2)][ClO_4]$ (4[ClO_4]). Yield: 71 mg (70%); M.p.: 348−350 °C (decomp.); IR (KBr disk): $\bar{\nu}$/cm^{-1} = 1652 s [$\nu_{as}(RCO_2^-)$], 1388 s [$\nu_s(RCO_2^-)$], 1217 s, 783 s [ν(C−Cl)], 716 s [ν(C−Cl)]; UV/vis (MeCN): λ_{max}/nm (ε/M^{-1} cm^{-1}) = 648 (25), 906 sh, 1098 nm (70). Elemental analysis (%) calcd. for $C_{40}H_{65}Cl_3N_6Ni_2O_6S_2$ (1013.86): C 47.39, H 6.46, N 8.29, S 6.33; found: C 47.28, H 6.42, N 8.05, S 6.41. **4**[BPh_4]: Yield: 113 mg (92%); Mp 286−288 °C (decomp.); Elemental analysis (%) calcd. for $C_{64}H_{85}BCl_2N_6Ni_2O_2S_2$ (1233.63): C 62.31, H 6.94, N 6.81, S 5.20; found: C 62.05, H 7.26, N 6.79, S 4.91; IR (KBr disk): $\bar{\nu}$/cm^{-1} = 1651 s [$\nu_{as}(RCO_2^-)$], 1389 s [$\nu_s(RCO_2^-)$], 784 br [ν(C−Cl)]; UV/vis (MeCN): λ_{max}/nm (ε/M^{-1} cm^{-1}) = 649 (34), 906 sh, 1100 (70).

$[Ni^{II}_2L(\mu\text{-}O_2CC{\equiv}CH)][ClO_4]$ (5[ClO_4]). Yield: 87 mg (91%); Mp 310−311 °C (decomp.); IR (KBr disk): $\bar{\nu}$/cm^{-1} = 3247 w [ν(H−C≡C)], 2097 w [ν(C≡C)], 1607 s [$\nu_{as}(RCO_2^-)$], 1375 s [$\nu_s(RCO_2^-)$]; UV/vis (MeCN): λ_{max}/nm (ε/M^{-1} cm^{-1}) = 653 (33), 907 sh, 1104 (78). Elemental analysis (%) calcd. for $C_{41}H_{65}ClN_6Ni_2O_6S_2$ (954.96): C 51.57, H 6.86, N 8.80, S 6.72; found: C 51.43, H 6.95, N 8.72, S 6.58. **5**[BPh_4]: Yield: 75 mg (64%); Mp 280−282 °C (decomp.); Elemental analysis (%) calcd. for $C_{65}H_{85}BN_6Ni_2O_2S_2$ (1174.74): C 66.46, H 7.29, N 7.15, S 5.46; found: C 66.48, H 7.55, N 6.90, S 5.21; IR (KBr disk): $\bar{\nu}$/cm^{-1} = 3304, 3281 w [ν(H−CC)], 2101 w [ν(C≡C)], 1607 s [$\nu_{as}(RCO_2^-)$], 1376 s [$\nu_s(RCO_2^-)$]; UV/vis (MeCN): λ_{max} (ε) = 654 (40), 906 sh, 1104 (76). This compound was additionally characterized by X-ray crystal structure analysis.

$[Ni^{II}_2L(\mu\text{-}O_2CCH_2Cl)][ClO_4]$ (6[ClO_4]). Yield: 69 mg (70%); Mp 352−354 °C (decomp.); IR (KBr disk): $\bar{\nu}$/cm^{-1} = 1624 s [$\nu_{as}(RCO_2^-)$], 1406 s [ν_s (RCO_2^-)], 784 m [ν(C−Cl)], 691 m [ν(C−Cl)]; UV/vis (MeCN): λ_{max}/nm (ε/M^{-1} cm^{-1}) = 650 (37), 904 sh, 1107 (76). Elemental analysis (%) calcd. for $C_{40}H_{66}Cl_2N_6Ni_2O_6S_2$ (979.41): C 49.05, H 6.79, N 8.58, S 6.55; found: C 49.11, H 6.83, N 8.55, S 6.48. **6**[BPh_4]: Yield: 102 mg (85%); Mp 298−300 °C (decomp.); Elemental analysis (%) calcd. for $C_{64}H_{86}BClN_6Ni_2O_2S_2$ (1199.19): C 64.10, H 7.23, N 7.01, S 5.35; found: C 63.99, H 7.50, N 6.92, S 4.86; IR (KBr disk): $\bar{\nu}$/cm^{-1} = 1624 [$\nu_{as}(RCO_2^-)$], 1409 [$\nu_{symm}(RCO_2^-)$]; UV/vis (MeCN): λ_{max}/nm (ε/M^{-1} cm^{-1}) = 650 (30), 905 sh, 1111 (72).

$[Ni^{II}_2L(\mu\text{-}O_2C{-}C_6H_4\text{-}pNO_2)][ClO_4]$ (7[ClO_4]). Yield: 61 mg (58%); M.p.: 356−358 °C (decomp.); IR (KBr disk): $\bar{\nu}$/cm^{-1} = 1621 m [ν(C=C)], 1590 s [$\nu_{as}(RCO_2^-)$], 1405 s [$\nu_s(RCO_2^-)$], 1522 s [$\nu_{as}(RNO_2)$], 1344 m [$\nu_s(RNO_2)$], UV/vis (MeCN): λ_{max}/nm (ε/M^{-1} cm^{-1}) = 650 (57), 911 sh, 1110 (78). Elemental analysis (%) calcd. for $C_{45}H_{68}ClN_7Ni_2O_8S_2$ (1052.03): C 51.37, H 6.51, N 9.32, S 6.10; found: C 51.16, H 6.37, N 9.25, S 5.84. **7**[BPh_4]: Yield 102 mg (80%). Mp 328−330 °C (decomp.). Elemental analysis (%) calcd for $C_{69}H_{88}BN_7Ni_2O_4S_2$ (1271.81): C 65.16, H 6.97, N 7.71, S 5.04; found: C 65.29, H 7.08, N 7.47, S 4.87; IR (KBr disk): $\bar{\nu}$/cm^{-1} = 1619 [ν(C=C)], 1588 [$\nu_{as}(RCO_2^-)$], 1404 [$\nu_s(RCO_2^-)$], 1521 [$\nu_{as}(RNO_2)$], 1344 [$\nu_s(RNO_2)$]; UV/vis (MeCN): λ_{max}/nm (ε/M^{-1} cm^{-1}) = 651 (48), 911 sh, 1110 (68).

(42) If not otherwise indicated, the values for the dissociation constants were taken from: Kortüm, G.; Vogel, W.; Andrussow, K. *Pure Appl. Chem.* **1960**, *1*, 187–536.

(43) Siebert, H.; Tremmel, G. *Z. Anorg. Allg. Chem.* **1972**, *390*, 292–302.
(44) Spinner, E. *J. Chem. Soc.* **1964**, 4217–4226.
(45) Lever, A. B. P; Odgen, D. *J. Chem. Soc.* **1967**, 2041–2048.
(46) Mansfield, C. H.; Whiting, M. C. *J. Chem. Soc.* **1956**, 4761–4764.
(47) Katon, J. E.; McDevitt, N. T. *Spectrochim. Acta* **1965**, *21*, 1717–1724.
(48) Dunn, G. E.; McDonald, R. S. *Can. J. Chem.* **1969**, *47*, 4577–4588.
(49) Newman, R. *J. Chem. Phys.* **1952**, *20*, 1663–1664.
(50) Matsue, T.; Evans, D. H.; Osa, T.; Kobayashi, N. *J. Am. Chem. Soc.* **1985**, *107*, 3411–3417.

[$Ni^{II}_2L(\mu\text{-}O_2CCH{=}CH_2)$][$ClO_4$] (12[$ClO_4$]). Yield: 61 mg (64%); Mp 213-216 °C (decomp.); IR (KBr disk): $\bar{\nu}/cm^{-1}$ = 1638 s [ν(C=C)], 1580 s [$\nu_{as}(RCO_2^-)$], 1428 m [$\nu_s(RCO_2^-)$]; UV/vis (MeCN): λ_{max}/nm ($\varepsilon/M^{-1}\,cm^{-1}$) = 652 (36), 907 sh, 1120 (75). Elemental analysis (%) calcd. for $C_{41}H_{67}ClN_6Ni_2O_6S_2$ (956.98): C 51.46, H 7.06, N 8.78, S 6.70; found: C 51.33, H 6.91, N 9.02, S 6.54. **12[BPh_4]**: Yield: 94 mg (80%); Mp 193−195 °C (decomp.); Elemental analysis (%) calcd. for $C_{65}H_{87}BN_6Ni_2O_2S_2$ (1176.75): C 66.34, H 7.45, N 7.14, S 5.45; found: C 66.29, H 7.32, N 6.92, S 5.38; IR (KBr disk): $\bar{\nu}/cm^{-1}$ = 1637 [ν(C=C)], 1578 [$\nu_{as}(RCO_2^-)$], 1428 [$\nu_s(RCO_2^-)$]; UV/vis (MeCN): λ_{max}/nm ($\varepsilon/M^{-1}\,cm^{-1}$) = 651 (42), 907 sh, 1122 (77).

[$Ni^{II}_2L(\mu\text{-}O_2CC_6H_4\text{-}pCH_3)$][$ClO_4$] (13[$ClO_4$]). Yield: 66 mg (65%); M.p.: 360−362 °C (decomp.); IR (KBr disk): $\bar{\nu}/cm^{-1}$ = 1615 w, 1596 m, 1587 w [ν(C=C)], 1562 s [$\nu_{as}(RCO_2^-)$], 1424 w, 1403 m [$\nu_s(RCO_2^-)$]; UV/vis (MeCN): λ_{max}/nm ($\varepsilon/M^{-1}\,cm^{-1}$) = 652 (30), 907 sh, 1121 (70)). Elemental analysis (%) calcd. for $C_{46}H_{71}ClN_6Ni_2O_6S_2$ (1021.06): C 54.11, H 7.01, N 8.23, S 6.28; found: C 54.26, H 7.27, N 8.34, S 6.13. **13[BPh_4]**: Yield: 108 mg (87%); M.p.: 290−292 °C (decomp.); Elemental analysis (%) calcd. for $C_{70}H_{91}BN_6Ni_2O_2S_2$ (1240.84): C 67.76, H 7.39, N 6.77, S 5.17; found: C 67.48, H 7.34, N 6.72, S 5.22; IR (KBr disk): $\bar{\nu}/cm^{-1}$ = 1613 w, 1594 sh, 1587 s [ν(C=C)], 1560 s [$\nu_{as}(RCO_2^-)$], 1426 m, 1403 m [ν_s (RCO_2^-)]; UV/vis (MeCN): λ_{max}/nm ($\varepsilon/M^{-1}\,cm^{-1}$) = 650 (44), 910 sh, 1122 (78).

[$Ni^{II}_2L(\mu\text{-}trans\text{-}O_2CCH{=}CHMe)$][$ClO_4$] (16[$ClO_4$]). Yield: 71 mg (73%); M.p.: 356−358 °C (decomp.); IR (KBr disk): $\bar{\nu}/cm^{-1}$ = 1661 m [ν(C=C)], 1575 s, [$\nu_{as}(RCO_2^-)$], 1413 s [$\nu_s(RCO_2^-)$]; UV/vis (MeCN): λ_{max}/nm ($\varepsilon/M^{-1}\,cm^{-1}$) = 655 (40), 905 sh, 1122 nm (72). Elemental analysis (%) calcd. for $C_{42}H_{69}ClN_6Ni_2O_8S_2$ (971.00): C 51.95, H 7.16, N 8.65, S 6.60; found: C 51.76, H 7.07, N 8.56, S 6.48. **16[BPh_4]:** Yield: 107 mg (90%); Mp 308−310 °C (decomp.); Elemental analysis (%) calcd. for $C_{66}H_{89}BN_6Ni_2O_2S_2$ (1190.78): C 66.57, H 7.53, N 7.06, S 5.39; found: C 66.50, H 7.69, N 6.90, S 5.12; IR (KBr disk): $\bar{\nu}/cm^{-1}$ = 1659 m [ν(C=C)], 1573 s, [$\nu_{as}(RCO_2^-)$], 1413 s [$\nu_s(RCO_2^-)$]; UV/vis (MeCN): λ_{max}/nm ($\varepsilon/M^{-1}\,cm^{-1}$) = 657 (45), 902 sh, 1129 (78).

[$Ni^{II}_2L(\mu\text{-}O_2CCH_2CH_3)$][$ClO_4$] (18[$ClO_4$]). Yield: 79 mg (82%); Mp > 300 °C (decomp.); IR (KBr disk): $\bar{\nu}/cm^{-1}$ = 1585 [$\nu_{as}(RCO_2^-)$], 1424 [$\nu_s(RCO_2^-)$]; UV/vis (MeCN): λ_{max}/nm ($\varepsilon/M^{-1}\,cm^{-1}$) = 650 (22), 903 sh, 1129 (63). Elemental analysis (%) calcd. for $C_{41}H_{69}ClN_6Ni_2O_6S_2$ (958.99): C 51.35, H 7.25, N 8.76, S 6.69; found: C 51.52, H 7.36, N 8.64, S 6.34; **18[BPh_4]:** Yield: 91 mg (77%); Mp 290−292 °C (decomp.); Elemental analysis (%) calcd for $C_{65}H_{89}BN_6Ni_2O_2S_2$ (1178.77): C 66.23, H 7.61, N 7.13, S 5.44; found: C 66.44, H 7.52, N 7.01, S 5.23; IR (KBr disk): $\bar{\nu}$ = 1583 [$\nu_{as}(CO_2)$], 1426 cm^{-1} [$\nu_s(CO_2)$]; UV/vis (MeCN): λ_{max}/nm ($\varepsilon/M^{-1}\,cm^{-1}$) = 651 (24), 907 sh, 1130 (66).

[$Ni^{II}_2L(\mu\text{-}O_2CC_{10}H_{15})$][$ClO_4$] (19[$ClO_4$]). Yield: 83 mg (78%); Mp 356−358 °C (decomp.); IR (KBr disk): $\bar{\nu}/cm^{-1}$ = 1567 s [$\nu_{as}(RCO_2^-)$], 1410 s [$\nu_s(RCO_2^-)$]; UV/vis (MeCN): λ_{max}/nm ($\varepsilon/M^{-1}\,cm^{-1}$) = 653 (29), 907 sh, 1122 (65). Elemental analysis (%) calcd. for $C_{49}H_{79}ClN_7Ni_2O_6S_2$ (1065.16): C 55.25, H 7.48, N 7.89, S 6.02; found: C 54.96, H 7.35, N 7.65, S 5.89. **19[BPh_4]:** Yield: 112 mg (87%); Mp 354−356 °C (decomp.); Elemental analysis (%) calcd. for $C_{73}H_{99}BN_6Ni_2O_2S_2$ (1284.93): C 68.24, H 7.77, N 6.54, S 4.99; found: C 68.32, H 7.83, N 6.38, S 4.86; IR (KBr disk): $\bar{\nu}/cm^{-1}$ = 1567 s [$\nu_{as}(RCO_2^-)$], 1410 s [$\nu_s(RCO_2^-)$]; UV/vis (MeCN): λ_{max}/nm ($\varepsilon/M^{-1}\,cm^{-1}$) = 650 (41), 1122 (75). This compound was additionally characterized by X-ray crystal structure analysis.

Carboxylate Exchange Reactions. All experiments were carried out with a 10-fold molar excess of the sodium or triethylammonium carboxylate at 50 °C. In a typical experiment, a solution of complex **8** (93 mg, 0.100 mmol) and sodium adamantate (202 mg, 1.00 mmol) in MeCN/MeOH (1:1, 100 mL) was stirred at 50 °C. Samples (5 mL) of the reaction mixture were removed at regular intervals (2 h, 4 h, 8 h). $LiClO_4 \cdot 3H_2O$ (100 mg, 0.623 mmol) was added, and the sample solution was concentrated under reduced pressure. The resulting solid was isolated by filtration, washed with EtOH, dried in vacuo, and then analyzed by IR spectroscopy. The relative amounts of the starting material and product were estimated from the relative intensities of the characteristic ν_{as}(CO) signals. This procedure was carried out twice to give reproducible values for the reaction rates. However, given the uncertainty of the integration method, the rate data presented in Table 5 below should be taken as indicative rather than definite.

Collection and Reduction of X-ray Data. Crystals of **2**[BPh_4]·MeCN, **3**[BPh_4]·2MeCN·EtOH, **5**[BPh_4]·1.5MeCN, and **19**[BPh_4]·3MeCN suitable for X-ray crystallographic analysis were obtained by slow evaporation of mixed MeCN/EtOH (1:1) solutions. The crystals were removed from the mother liquor and immediately immersed in a drop of perfluoropolyether oil. A suitable crystal was selected, attached to a glass fiber, and placed in a low-temperature nitrogen stream of the diffractometer. All data were collected at 213(2) K using a Bruker AXS diffractometer or a STOE IPDS I diffractometer (for **2**) equipped with Mo Kα radiation.[54] Absorption corrections were applied using the Sadabs program.[55] The structures were solved by Direct Methods[56] and refined by full-matrix least-squares on the basis of all data against F^2 using Shelxl-97.[57] The program Platon was used to search for higher symmetry.[58] All non-hydrogen atoms were refined anisotropically. Split atom models were used to account for disorder of the CF_3 and *tert*-butyl groups in complexes **2**, **3**, **5**, and **19** using the SADI instructions implemented in the Shelxtl program suite. The site occupancies of the two positions were refined as follows: F(1a)-F(3a)/F(1b)-F(3b) 0.51(2)/0.49(1) and C(32a)-C(34a)/C(32b)-C(34b) 0.60(2)/0.40(2) for **2**; C(32a)-C(34a)/C(32b)-C(34b) 0.70(3)/0.30(3) and C(36a)-C(38a)/C(36b)-C(38b) 0.53(1)/0.47(1) for **5**; C(36a)-C(38a)/C(36b)-C(38b) 0.58(1)/0.42(1) for **19**. In the structure of **19**, one MeCN molecule was found to be disordered over two positions. The site occupancies of the two positions were refined as follows: N(9)C(54)C(55a)/N(9)C(54)C(55b) 0.79(4)/0.21(4). In the crystal structure of **3**[BPh_4]·2MeCN·EtOH, the C and O atoms of the EtOH solvate molecule were refined isotropically. H atoms were placed at calculated positions and refined as riding atoms with isotropic displacement parameters. Selected details of the data collection and refinement are given in Table 3. Drawings were produced with Ortep 3 for Windows.[59]

Results and Discussion

Preparation of the Metal Complexes. Table 1 lists the synthesized complexes and their labels. Several of these have been reported previously, as for instance the formato (**8**),[22] 2-chlorobenzoato (**9**),[60] ferrocene

(51) Wu, H.; Gao, Y.; Yu, K. *Transition Met. Chem.* **2004**, *29*, 175–179.
(52) Zelenák, V.; Vargová, Z.; Györyová, K. *Spectrochim. Acta A* **2007**, *66*, 262–272.
(53) Pethybridge, A. H.; Ison, R. W.; Harrigan, W. F. *J. Food Technol.* **1983**, *18*, 789–796.
(54) *ShelXTL*, version 5.10; Bruker AXS: Madison, WI, 1998.
(55) *SADABS, an empirical absorption correction program part ot the SAINTPlus NT version 5.0 package*; Bruker AXS: Madison, WI, 1998.
(56) Sheldrick, G. M. *Acta Crystallogr.* **1990**, *A46*, 467–473.
(57) Sheldrick, G. M. *Shelxl-97, Computer program for crystal structure refinement*; University of Göttingen: Göttingen, Germany, 1997.
(58) Spek, A. L. *Platon - A Multipurpose Crystallographic Tool*; Utrecht University: Utrecht, The Netherlands, 2000.
(59) Farrugia, L. J. *J. Appl. Crystallogr.* **1997**, *30*, 565.
(60) Hausmann, J.; Käss, S.; Klod, S.; Kleinpeter, E.; Kersting, B. *Eur. J. Inorg. Chem.* **2004**, 4402–4411.

Table 1. Synthesized Complexes, Their Labels, and Selected IR and UV/vis Spectroscopic Data

	compound	pK_b[42]	ν_{as}, ν_s; Δ/cm^{-1} [a]	ν_2, ν_1/nm; Δ_o/cm^{-1} [b]
1[c]	$[Ni^{II}_2L(\mu\text{-}Cl)]^+$			
2[d]	$[Ni^{II}_2L(\mu\text{-}O_2CCF_3)]^+$	13.77	1684, 1348; 336 [1682, 1442; 240][43]	646, 1094; 9141
3[d]	$[Ni^{II}_2L(\mu\text{-}O_2CCCl_3)]^+$	13.34	1683, 1349; 334 [1677, 1353; 324][44]	649, 1088; 9191
4	$[Ni^{II}_2L(\mu\text{-}O_2CCHCl_2)]^+$	12.74	1652, 1388; 264 [1629, 1370; 259][45]	648, 1098; 9107
5[d]	$[Ni^{II}_2L(\mu\text{-}O_2CC{\equiv}CH)]^+$	12.16[46]	1607, 1375; 232 [1600, 1382; 218][47]	653, 1104; 9058
6	$[Ni^{II}_2L(\mu\text{-}O_2CCH_2Cl)]^+$	11.18	1624, 1406; 218 [1595, 1405; 190][45]	650, 1107; 9033
7	$[Ni^{II}_2L(\mu\text{-}O_2CC_6H_4\text{-}p\text{-}NO_2)]^+$	10.55	1590, 1405; 185 [1575, 1392; 183][48]	650, 1110; 9009
8[c]	$[Ni^{II}_2L(\mu\text{-}O_2CH)]^+$	10.25	1603, 1369; 234 [1620, 1377; 243][49]	651, 1114; 8977
9[c]	$[Ni^{II}_2L(\mu\text{-}O_2CC_6H_4\text{-}m\text{-}Cl)]^+$	10.18	1565, 1392; 173 [1554, 1384; 170][48]	651, 1116; 8961
10[c]	$[Ni^{II}_2L(\mu\text{-}O_2C(C_5H_4)FeCp]^+$	9.80[50]	1571, 1425; 146 [1548, 1393; 155][g]	649, 1112; 8992
11[c]	$[Ni^{II}_2L(\mu\text{-}O_2CPh)]^+$	9.80	1569, 1407; 162 [1548, 1391; 157][48]	651, 1120; 8929
12	$[Ni^{II}_2L(\mu\text{-}O_2CCH{=}CH_2)]^+$	9.75	1580, 1428; 152 [1560, 1428; 132][51]	652, 1120; 8929
13	$[Ni^{II}_2L(\mu\text{-}O_2CC_6H_4\text{-}pCH_3)]^+$	9.63	1562, 1403; 159 [1542, 1389; 153][48]	652, 1121; 8921
14[c]	$[Ni^{II}_2L(\mu\text{-}O_2CCH{=}CHPh)]^+$	9.56	1578, 1406; 172 [1551, 1408; 143][52]	654, 1125; 8889
15[c]	$[Ni^{II}_2L(\mu\text{-}O_2C(CH{=}CH)_2CH_3)]^+$	9.33[53]	1567, 1395; 172 [1563, 1424; 141][g]	650, 1120; 8929
16	$[Ni^{II}_2L(\mu\text{-}O_2CCH{=}CHCH_3)]^+$	9.29	1575, 1413; 162 [1561, 1433; 128][g]	655, 1122; 8913
17[c]	$[Ni^{II}_2L(\mu\text{-}O_2CCH_3)]^+$	9.24	1588, 1428; 160 [1578, 1414; 164][45]	651, 1128; 8865
18	$[Ni^{II}_2L(\mu\text{-}O_2CCH_2CH_3)]^+$	9.11	1585, 1424; 161 [1558, 1416; 142][45]	648, 1129; 8857
19[d]	$[Ni^{II}_2L(\mu\text{-}O_2CC_{10}H_{15})]^{+e}$	9.10[f]	1567, 1410; 157 [1555, 1408; 147][g]	653, 1122; 8913
20[c]	$[Ni^{II}_2L(\mu\text{-}O_2CR')]^{+e}$	9.10[f]	1573, 1400; 173 [n.d.][h]	650, 1112; 8993

[a] The data correspond to the ClO_4^- salts (see Experimental Section for the BPh_4^- salts); $\Delta = \nu_{as} - \nu_s$; values in square brackets refer to the corresponding sodium carboxylates. [b] Values obtained from about 10^{-3} M solutions of the ClO_4^- salts in MeCN (see Experimental Section for the values of the BPh_4^- salts). [c] The crystal structure of this compound was reported previously. [d] The crystal structure of this compound is reported in this study. [e] $C_{10}H_{15}CO_2^-$ = adamantate, $R'CO_2^-$ = 3,4-dimethyl-6-phenylcyclohex-3-ene carboxylate. [f] Estimated values. [g] Determined in this work. [h] Not determined.

monocarboxylato (**10**),[61] benzoato (**11**),[16] cinnamato (**14**),[40] sorbato (**15**),[40] acetato (**17**),[17] and 3,4-dimethyl-6-phenylcyclohex-3-ene carboxylato bridged compounds (**20**).[40] The other carboxylato complexes in Table 1 were prepared in a similar fashion (eq 1) by treatment of the chloro complex $[Ni^{II}_2L(\mu\text{-}Cl)][ClO_4]$ **1**,[15] with a slight excess of the sodium or triethylammonium salt of the corresponding carboxylate anion, prepared in situ from the free acid and a base, in methanol at ambient temperature. The complexes could be readily isolated as perchlorate salts and were subsequently subjected to anion metathesis with $NaBPh_4$ to generate the corresponding tetraphenylborate salts (eq 2). The reaction in eq 1 does not appear to be affected by the varying basicity or the steric hindrance of the respective carboxylate ion, as all complexes are obtained in equally good yields of about 70−90% (unoptimized). It should be noted that $[Ni^{II}_2L(\mu\text{-}O_2CR)]^+$ complexes are less readily prepared by carboxylate exchange reactions (see further below), which contrasts the behavior of the related zinc(II) complexes.

$$[Ni^{II}_2L(\mu\text{-}Cl)][ClO_4] + NaO_2CR \text{ (or } [NEt_3H]O_2CR) \rightarrow [Ni^{II}_2L(\mu\text{-}O_2CR)][ClO_4] + NaCl \text{ (or } [NEt_3H]Cl) \quad (1)$$

$$[Ni^{II}_2L(\mu\text{-}O_2CR)][ClO_4] + NaBPh_4 \rightarrow [Ni^{II}_2L(\mu\text{-}O_2CR)][BPh_4] + NaClO_4 \quad (2)$$

All compounds are stable in air, both in solution and in the solid state. The ClO_4^- salts exhibit good solubility in polar aprotic solvents such as MeCN, acetone, and dichloromethane, but are not very soluble in alcohols and virtually insoluble in water. The BPh_4^- salts could be obtained as pale-green crystals by slow evaporation from a mixed MeCN/EtOH (1:1) solvent system. The products thus purified gave satisfactory elemental analyses and were characterized by IR and UV/vis spectroscopy and by X-ray structure analysis (**2**$[BPh_4]\cdot$MeCN,

(61) Lozan, V.; Buchholz, A.; Plass, W.; Kersting, B. *Chem.—Eur. J.* **2007**, *13*, 7305–7316.

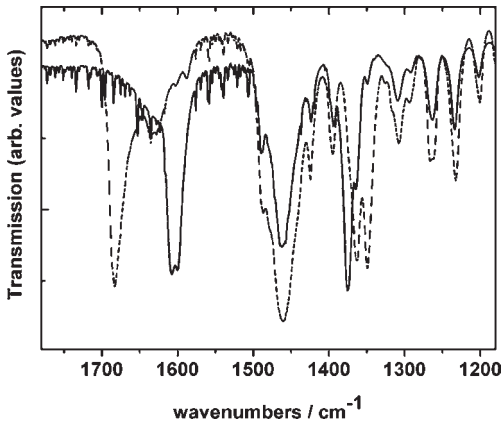

Figure 1. Overlay of the IR spectra of **3**[ClO_4] (dashed line) and **5**[ClO_4] (solid line).

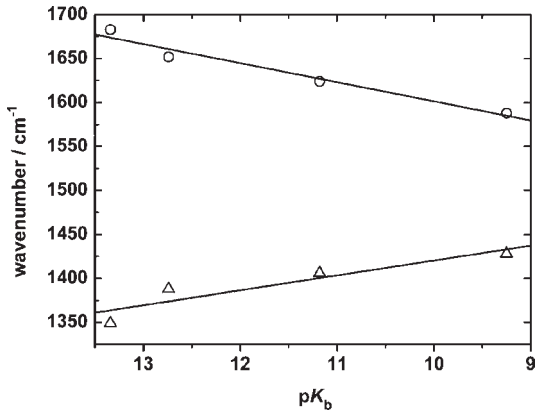

Figure 2. Plot of ν_{as} (open circles) and ν_s (open triangles) for complexes **3**, **4**, **6**, and **17** versus the pK_b value of the corresponding carboxylato ligands.

3[BPh_4]·2MeCN·EtOH, **5**[BPh_4]·1.5MeCN, and **19**[BPh_4]·3MeCN).[62]

Spectroscopic Characterization of the Complexes. Infrared Spectroscopy. The carboxylate ion displays versatile coordination behavior,[27] and infrared (IR) spectroscopy is a powerful tool to distinguish between its different coordination modes.[63] In fact, the frequency of the asymmetric and symmetric C=O stretching modes, ν_{as} and ν_s, respectively, and their separation $\Delta = \nu_{as} - \nu_s$ are often used as spectroscopic criteria to identify the carboxylate binding mode.[43,64,65] A number of correlations between the carboxylate stretching frequencies and the carboxylate binding mode have been reported in the literature.[52,64,66−69] Nevertheless, there are only a few systematic IR spectroscopic studies of isostructural carboxylato complexes. Most of them involve inert cobalt(III) species.[43,70] To our knowledge, a systematic IR study of an isostructural series of carboxylato-bridged nickel(II) complexes has not been reported.[45,71]

FT-IR spectra of the dinuclear nickel(II) complexes **2**−**20** were recorded over the range 4000−400 cm^{-1}. Figure 1 shows the spectra of the two representative compounds **3** and **5** in the 1800−1200 cm^{-1} region. Assignments of the bands are based on comparisons between the individual complexes and on comparisons with the IR data for the respective sodium carboxylates (Table 1). In some cases, an unambiguous assignment could not be made, either because of poor resolution, low signal intensity, or superpositions of the signals.

Table 1 shows that the ν_{as} frequencies of the complexes (except **8**) are blue-shifted by up to 25 cm^{-1} relative to the sodium carboxylates, an observation that is consistent with the coordination of the RCO_2^- group to the $[Ni^{II}_2L]^{2+}$ fragment. Note that the ν_{as} and ν_s values of **2**−**20** differ by as much as 100 cm^{-1} (ν_{as} = 1684−1576 cm^{-1}, ν_s = 1428−1348 cm^{-1}). This scattering reflects the varying basicity of the respective carboxylate, since the immediate environment of the carboxylato group in all $[Ni^{II}_2L(\mu\text{-}O_2CR)]^+$ complexes is essentially the same. Indeed, there is a clear correlation between the frequencies and the carboxylate ion basicity. The frequency ν_{as} decreases while ν_s increases with increasing carboxylate basicity. A particularly good ν_{as} versus pK_b correlation exists for the trichloro-, dichloro-, chloro-, and acetato bridged complexes (i.e., **3**, **4**, **6**, and **17**) as they are structurally and electronically related. Here, the correlation is almost linear (Figure 2).

The observations and conclusions made for the present complexes are in line with those made for the free acids and other series of carboxylato complexes.[48,72,73] In fact, for the present complexes, the IR spectra of the nickel-bound carboxylato ligand are almost superimposable with those of the free sodium carboxylates, with the exception of the about 20−25 cm^{-1} blue-shift of the ν_{as} frequency.[74] These observations further suggest that the Δ criterion[63] should be used with care for assignment of carboxylato binding modes. The pK_b dependence of the separation $\Delta = \nu_{as} - \nu_s$ has to be taken into account.

UV/vis Spectroscopy. The complexes were further studied by electronic absorption spectroscopy to see whether the electronic transitions of the $[Ni^{II}_2L(\mu\text{-}O_2CR)]^+$ complexes correlate with the pK_b values of the carboxylato ligands. Electronic absorption spectra for all complexes were recorded in MeCN solution over the range 300−1600 nm. Figure 3 shows the spectra of MeCN solutions of two representative compounds (trichloroacetato complex **3** and acetato complex **17**) in the 500−1400 nm region. Table 1 lists selected values and their assignments.

The electronic absorption spectra of **2**−**20** are similar but not identical. Each complex exhibits two weak

(62) The thiolate complexes were also examined by cyclic voltammetry. However, their irreversible redox behavior prevented an analysis of the variation in redox potential as a function of pK_b.

(63) Nakamoto, K. *Infrared and Raman Spectra of Inorganic and Coordination Compounds*, 5th ed.; Wiley: New York, 1997.
(64) Deacon, G. B.; Philipp, R. J. *Coord. Chem. Rev.* **1980**, *33*, 227–250.
(65) Martini, D.; Pellei, M.; Pettinari, C.; Skelton, B. W.; White, A. H. *Inorg. Chim. Acta* **2002**, *333*, 72–82.
(66) Edsall, J. T. *J. Chem. Phys.* **1937**, *5*, 508–517.
(67) Lewandowski, W.; Kalinowska, M.; Lewandowska, H. *J. Inorg. Biochem.* **2005**, *99*, 1407–1423.
(68) Czakis-Sulikowska, D.; Czylkowska, A.; Malinowska, A. *J. Therm. Anal. Cal* **2002**, *67*, 667–678.
(69) (a) Ishioka, T.; Shibata, Y.; Takahashi, M.; Kanesaka, I.; Kitagawa, Y.; Nakamura, K. T. *Spectrochim. Acta* **1998**, *54A*, 1827–1836.
(70) Wieghardt, K. *J. Chem. Soc., Dalton Trans.* **1973**, 2548–2552.
(71) Kumar, N.; Kachroo, P. L.; Kant., R. *Bull. Chem. Soc. Jpn.* **1980**, *53*, 1787–1788.
(72) Lindberg, B. J. *Acta Chem. Scand.* **1968**, *22*, 571–580.
(73) Lloyd, H. A.; Warren, K. S.; Fales, H. M. *J. Am. Chem. Soc.* **1966**, *88*, 5544–5549.
(74) Shindo, H.; Brown, T. L. *J. Am. Chem. Soc.* **1965**, *87*, 1904–1909.

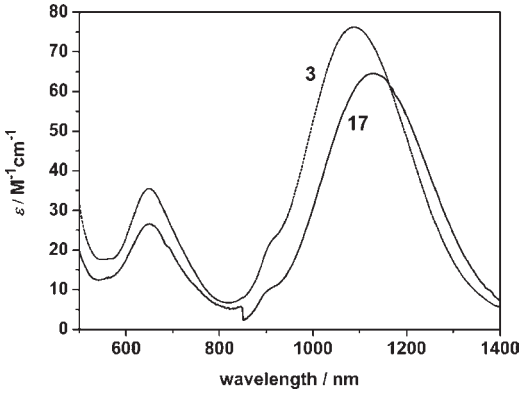

Figure 3. Electronic absorption spectra of **3**[ClO_4] and **17**[ClO_4] in MeCN at ambient temperature at about 10^{-3} M.

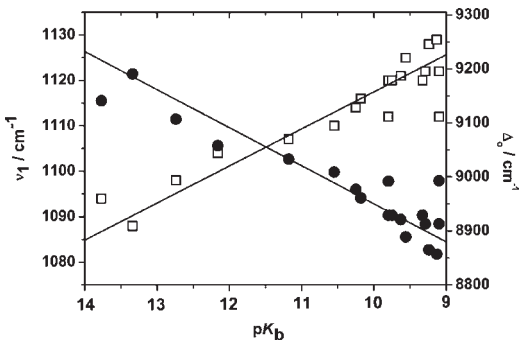

Figure 4. Plot of ν_1 (open squares) and Δ_o (full circles) versus pK_b for the complexes **2**−**20**. The pK_b values of the carboxylates in complexes **19** and **20** are estimated to be 4.90.

absorption bands in the 500−1600 nm region which can be assigned to the spin-allowed $^3A_{2g} \rightarrow {}^3T_{1g}$ (ν_2) and $^3A_{2g} \rightarrow {}^3T_{2g}$ (ν_1) transitions of a nickel(II) ($S = 1$) ion with O_h symmetry.[75] There is also a weak shoulder around 910 nm attributable to a spin-forbidden $^3A_{2g} \rightarrow {}^1E_g$(D) transition which gains intensity because of the lowering of the symmetry. The $^3A_{1g} \rightarrow {}^3T_{1g}$(P) transition (expected below 400 nm) is obscured in each case by the strong thiolato-nickel(II) LMCT transitions which occur in that same spectral region.

Figure 4 shows a plot of the ν_1 values for **2**−**20** against the pK_b value of the carboxylato ligands. As can be seen, the ν_1 values are steadily red-shifted with increasing carboxylate ion basicity, from 1094 nm in **2** bearing the weakly basic trifluoroacetate ion (pK_b = 14 − pK_a = 13.76) to 1129 nm in **18** with the much more basic propionate ion (pK_b = 9.11). No clear trend is observed for the ν_2 values, which scatter randomly between 546 and 555 nm.

Rough estimates of the octahedral splitting parameters Δ_o, which are inversely proportional to ν_1 (Δ_o [cm^{-1}] = $10^7/\nu_1$ [nm]),[75] can be obtained from the ν_1 transitions. Figure 4 shows that Δ_o decreases with increasing carboxylate basicity, from 9141 cm^{-1} in the trifluoroacetato complex **2** to 8857 cm^{-1} in the propionato complex **18**. This is somewhat surprising as the Ni−O bond weakening is observed upon going from **2** to **18** (vide infra). Given

(75) Lever, A. B. P. *Inorganic Electronic Spectroscopy*, 2nd ed.; Elsevier Science: Amsterdam, 1984.

Table 2. Selected UV/vis Data for $[Ni^{II}_2L(\mu\text{-}L')]^+$ Complexes[a]

complex	coligand	ν_2/nm	ν_1/nm	Δ_o/cm^{-1}	ref.
21[c,d]	NO_3^-	659 (46)	1049 (77)	9532	16
22[b]	ClO_4^-	578 (129)	1066 (86)	9381	18
23[c,d]	N_3^-	672 (37)	1092 (84)	9158	16
24[c,d]	*pydz* [e]	615 (33)	1095 (62)	9132	16
25[b]	S_6^{2-}	647 (56)	1102 (72)	9074	10
26[c,d]	NO_2^-	621 (40)	1111 (57)	9001	16
27	*phtz* [e]	629 (43)	1111 (57)	9001	16
28[c,d]	N_2H_4	624 (33)	1114 (67)	8977	16
8	O_2CH	651 (27)	1114 (86)	8977	this work
11	O_2CPh^-	651 (35)	1120 (66)	8929	this work
17	$O_2CCH_3^-$	651 (26)	1128 (65)	8865	this work
27[b]	SPh^-	667 (52)	1141 (68)	8764	10
28[b]	SH^-	663 (32)	1175 (49)	8511	10
29[c,d]	*pz* [e]	634 (23)	1180 (67)	8475	16

[a] In MeCN solution. [b] The data refer to the BPh_4^- salts. [c] The data refer to the ClO_4^- salts. [d] In MeOH solution. [e] *pydz* = pyridazine, *phtz* = phthalazine, *pz* = pyrazolate.

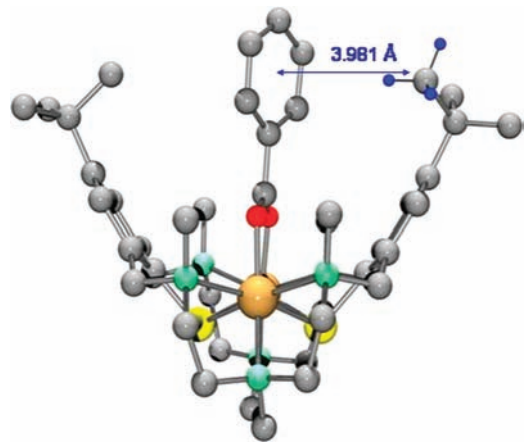

Figure 5. Secondary CH···π bonding interactions in the benzoato complex **11**. This figure was generated using data downloaded from The Cambridge Crystallographic Data Centre (CCDC) and corresponds to the structure originally reported in ref 16.

that Δ_o is determined by the complete N_3S_2O donor set and not just the O donors, it can be concluded that binding of a basic carboxylate donor weakens the macrocycle-nickel(II) interactions (i.e., the Ni−N and Ni−S bonds) and vice versa. This coupling of the Ni−O bonding interactions to the Ni−N and Ni−S −bonds is indeed reflected in small but consistent bond length changes across the series (vide infra). The UV/vis data for other previously characterized $[Ni^{II}_2L(\mu\text{-}L')]^+$ complexes are also in line with this assumption. Table 2 lists some representative examples ordered by decreasing Δ_o values. As discussed above, the $[Ni^{II}_2L(\mu\text{-}L')]^+$ complexes bearing weakly basic coligands (such as the NO_3^- and ClO_4^- ions) feature the highest Δ_o values. Thus, as discussed above, the N_6S_2 macrocycle adapts to the bonding preferences of the coligand, which results in varying contributions of coligand and macrocycle to Δ_o.

It should be noted that no relationship exists between the Δ_o values and the relative binding affinity of the $[Ni^{II}_2L]^{2+}$ fragment for a certain coligand.[76,77] In a previous study, we determined the relative stabilities of some $[Ni^{II}_2L(\mu\text{-}L')]^+$ complexes by exchange experiments.[16] The relative stabilities of some of the compounds listed in Table 2 were determined as follows: benzoate > acetate > N_3^- > pyrazolate (*pz*) > NO_2^- > N_2H_4 > NO_3^- > phthalazine

Table 3. Selected Crystallographic Data for Compounds **2**[BPh_4]·MeCN, **3**[BPh_4]·2MeCN·EtOH, **5**[BPh_4]·1.5MeCN, and **19**[BPh_4]·3MeCN[a]

	2[BPh_4]·MeCN	**3**[BPh_4]·2MeCN·EtOH	**5**[BPh_4]·1.5MeCN	**19**[BPh_4]·3MeCN
formula	$C_{66}H_{87}BF_3N_7Ni_2O_2S_2$	$C_{70}H_{96}BCl_3N_8Ni_2O_3S_2$	$C_{68}H_{89.5}BN_{7.5}Ni_2O_2S_2$	$C_{79}H_{108}BN_9Ni_2O_2S_2$
formula weight [g/mol]	1259.78	1396.25	1236.32	1408.09
space group	$P\bar{1}$	$P\bar{1}$	$P2_1/n$	$P\bar{1}$
a, Å	13.385(2)	14.256(3)	19.208(4)	13.173(3)
b, Å	15.598(2)	17.082(3)	18.136(4)	16.845(3)
c, Å	17.406(2)	17.772(3)	20.086(4)	18.155(4)
α, deg	106.73(1)	116.10(1)	90.00	108.79(3)
β, deg	92.53(1)	109.19(1)	112.26(3)	95.30(3)
γ, deg	108.49(1)	94.80(1)	90.00	94.59(3)
V, Å^3	3263.4(9)	3535(1)	6476(2)	3772(1)
Z	2	2	4	2
$D_{calcd.}$, g/cm^3	1.282	1.312	1.268	1.240
cryst. size, mm^3	0.35 × 0.20 × 0.15	0.24 × 0.20 × 0.20	0.49 × 0.36 × 0.32	0.30 × 0.30 × 0.18
μ(Mo Kα), mm^{-1}	0.697	0.756	0.696	0.606
$R1$[b] ($R1$ all data)	0.0327 (0.0651)	0.0502 (0.1143)	0.0572 (0.2141)	0.0423 (0.1012)
w$R2$[c] (w$R2$ all data)	0.0597 (0.0692)	0.1055 (0.1296)	0.1149 (0.1678)	0.0839 (0.1023)
Max, min peaks, e/Å^3	0.532/−0.252	0.871/ −0.682	0.523/−0.825	0.602/−0.591

[a] Observation criterion: $I > 2\sigma(I)$. [b] $R1 = \sum||F_o| - |F_c||/\sum|F_o|$. [c] $wR2 = \{\sum w(F_o^2 - F_c^2)^2/\sum w(F_o^2)^2\}^{1/2}$.

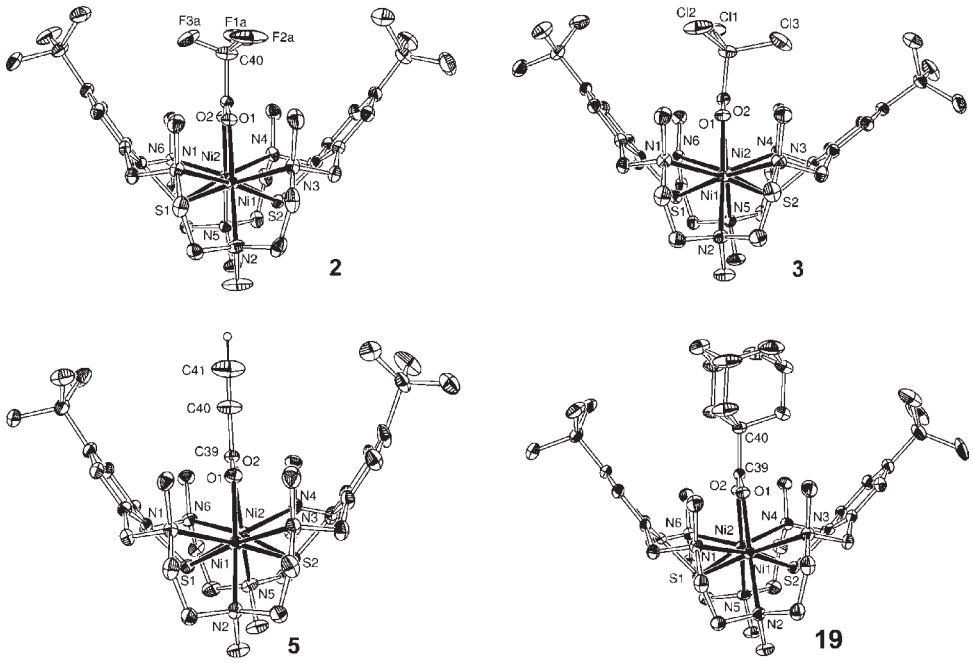

Figure 6. ORTEP views of the structures of the cations $[Ni^{II}_2L(\mu\text{-}O_2CCF_3)]^+$ (**2**), $[Ni^{II}_2L(\mu\text{-}O_2CCCl_3)]^+$ (**3**), $[Ni^{II}_2L(\mu\text{-}O_2CC{\equiv}CH)]^+$ (**5**), and $[Ni^{II}_2L(\mu\text{-}O_2CC_{10}H_{15})]^+$ (**19**). Thermal ellipsoids are drawn at the 30% probability level. Hydrogen atoms, except the terminal hydrogen atom of the propiolato coligand in **5**, have been omitted for clarity. For rotationally disordered CF_3 and/or *t*Bu groups only one orientation is displayed.

> (*phtz*) > pyridazine (*pz*) > ClO_4^-. Inspection of the corresponding data clearly shows that a correlation between the complex stabilities and the Δ_o values does not exist. Otherwise, the ClO_4^- complex (which has the highest Δ_o) would be the most stable complex, but this is definitely not the case.

Another fact worth considering here is the fact that complex stability differences due to secondary bonding interactions such as CH···π interactions[78] between the organic residues of the supporting ligand and the coligand, as seen in the set of $[Zn^{II}_2L(\mu\text{-}O_2CR)]^+$ complexes,[17,40] are not reflected in the Δ_o values of the present $[Ni^{II}_2L(\mu\text{-}O_2CR)]^+$ compounds. Thus, the relative stability constants for the formato-, acetato-, and benzoato-bridged nickel(II) complexes, estimated from carboxylate exchange reactions (vide infra), increase in the order formato (**8**) < acetato (**17**) < benzoato (**11**), but this ranking is not reflected in the Δ_o values.

(76) The UV/vis spectral data of **2**−**18** may be used to estimate a relative stability difference of the $[Ni_2^{II}L(\mu\text{-}O_2CR)]^+$ complexes. As the complexes are structurally very similar, one simply needs to determine the difference of the ligand field stabilization energies (which contributes to the stability of a transition metal complex) across the series (if it can be assumed that all other effect cancel out). For the present nickel(II) complexes with a d^8 electronic configuration ($t_{2g}^6e_g^2$, $S = 1$), LFSE(Ni^{2+}) = 1.2 × Δ_o. Thus, by taking complexes **2** and **18** as pivots, the difference $\Delta_{LFSE(2,18)}$ = LFSE(**2**) − LFSE(**18**) = 1.2 × (9141 cm^{-1} − 8857 cm^{-1}) × 11.96 J/(mol cm^{-1}) = 4.08 kJ/mol. This is a small value.

(77) Holleman, A. F.; Wiberg, N. *Lehrbuch der Anorganischen Chemie*; Walter de Gruyter: Berlin, 2007; Vol. *102*, pp 1327−1363.

(78) Meyer, E. A.; Castellano, R. K.; Diederich, F. *Angew. Chem.* **2003**, *115*, 1244–1287. Meyer, E. A.; Castellano, R. K.; Diederich, F. *Angew. Chem., In. Ed.* **2003**, *42*, 1210–1250.

Table 4. Selected Bond Lengths [Å] and Angles [deg] in the $[Ni^{II}_2L(\mu\text{-}O_2CR)]^+$ Cations in Crystals of **2**[BPh_4]·MeCN, **3**[BPh_4]·2MeCN·EtOH, **5**[BPh_4]·1.5MeCN, **8**[BPh_4],[22] **10**[BPh_4]·MeCN,[61] **11**[BPh_4],[16] **15**[BPh_4],[40] **17**[BPh_4]·MeCN,[17] **19**[BPh_4]· and **20**[BPh_4]·2MeCN[40]

	2	**3**	**5**	**8**[a]	**9**[a]	**10**	**11**[a]	**15**	**17**	**19**	**20**
Ni(1)−O(1)	2.035(2)	2.014(2)	2.014(4)	1.992(4) [2.000(4)]	2.010(3) [2.028(3)]	2.021(5)	2.007(2) [1.995(2)]	2.011(3)	1.998(2)	2.003(2)	2.043(2)
Ni(1)−N(1)	2.256(2)	2.277(3)	2.247(4)	2.255(5) [2.238(6)]	2.282(3) [2.281(3)]	2.323(5)	2.322(3) [2.207(3)]	2.292(3)	2.281(2)	2.269(2)	2.285(2)
Ni(1)−N(2)	2.145(2)	2.136(3)	2.127(4)	2.146(5) [2.167(5)]	2.176(4) [2.158(3)]	2.168(6)	2.137(3) [2.123(3)]	2.162(3)	2.152(2)	2.152(2)	2.173(2)
Ni(1)−N(3)	2.256(2)	2.255(3)	2.284(5)	2.266(6) [2.313(6)]	2.222(4) [2.239(3)]	2.233(5)	2.197(3) [2.342(3)]	2.243(3)	2.251(2)	2.266(2)	2.223(2)
Ni(1)−S(1)	2.5165(7)	2.489(1)	2.498(2)	2.497(2) [2.501(2)]	2.504(2) [2.512(1)]	2.503(2)	2.452(1) [2.493(2)]	2.495(1)	2.493(1)	2.490(1)	2.480(1)
Ni(1)−S(2)	2.4663(7)	2.453(1)	2.460(2)	2.477(2) [2.466(2)]	2.406(2) [2.396(1)]	2.408(2)	2.509(2) [2.452(1)]	2.438(1)	2.448(1)	2.423(1)	2.4487(8)
Ni(2)−O(2)	2.053(2)	2.033(3)	2.012(4)	1.996(4) [2.000(4)]	2.020(3) [2.016(3)]	2.016(4)	2.004(2) [2.013(2)]	1.999(3)	2.008(2)	2.010(2)	1.994(2)
Ni(2)−N(4)	2.243(2)	2.214(3)	2.221(4)	2.243(6) [2.250(6)]	2.207(4) [2.216(3)]	2.218(5)	2.274(3) [2.202(3)]	2.237(3)	2.244(2)	2.253(2)	2.265(2)
Ni(2)−N(5)	2.155(2)	2.166(3)	2.135(5)	2.136(6) [2.135(6)]	2.170(4) [2.172(3)]	2.176(5)	2.133(3) [2.166(3)]	2.151(3)	2.158(2)	2.155(2)	2.159(2)
Ni(2)−N(6)	2.288(2)	2.294(3)	2.329(4)	2.320(6) [2.319(6)]	2.307(4) [2.311(3)]	2.298(5)	2.259(3) [2.338(3)]	2.307(3)	2.295(2)	2.286(2)	2.293(2)
Ni(2)−S(1)	2.4957(8)	2.499(1)	2.477(2)	2.487(2) [2.479(2)]	2.484(2) [2.501(2)]	2.512(2)	2.506(2) [2.441(1)]	2.504(2)	2.493(1)	2.476(1)	2.4982(7)
Ni(2)−S(2)	2.4731(7)	2.446(1)	2.472(2)	2.478(2) [2.488(2)]	2.401(1) [2.398(1)]	2.417(2)	2.445(1) [2.485(1)]	2.433(1)	2.450(1)	2.437(1)	2.4256(9)
O(1)−C(39)	1.242(2)	1.235(4)	1.246(6)	1.272(7) [1.256(7)]	1.257(5) [1.258(4)]	1.242(8)	1.258(4) [1.251(4)]	1.263(4)	1.249(3)	1.264(3)	1.259(2)
O(2)−C(39)	1.250(2)	1.254(4)	1.253(6)	1.237(7) [1.266(7)]	1.255(5) [1.259(4)]	1.264(8)	1.250(4) [1.261(4)]	1.252(4)	1.252(3)	1.256(3)	1.255(2)
Ni−N[b]	2.224(2)	2.224(3)	2.224(4)	2.228(6) [2.237(6)]	2.227(4) [2.230(3)]	2.236(5)	2.220(3) [2.231(3)]	2.232(3)	2.230(2)	2.230(2)	2.233(2)
Ni−N[trans]	2.150(2)	2.151(3)	2.131(4)	2.141(6) [2.151(6)]	2.173(4) [2.165(3)]	2.172(6)	2.131(3) [2.146(3)]	2.157(2)	2.155(2)	2.154(2)	2.166(2)
Ni−O[b]	2.044(2)	2.024(2)	2.013(4)	1.994(4) [2.000(4)]	2.015(3) [2.022(3)]	2.019(5)	2.004(3) [2.004(2)]	2.005(3)	2.003(2)	2.007(3)	2.019(2)
Ni−S[b]	2.4879(7)	2.472(1)	2.477(2)	2.485(2) [2.484(2)]	2.448(2) [2.452(2)]	2.460(2)	2.478(2) [2.468(1)]	2.468(1)	2.471(2)	2.457(1)	2.4631(9)
O−C[b]	1.246(2)	1.245(4)	1.250(6)	1.255(7) [1.261(7)]	1.256(5) [1.259(2)]	1.253(8)	1.254(4) [1.256(4)]	1.258(4)	1.251(3)	1.260(3)	1.257(2)
Ni···Ni	3.553(1)	3.524(1)	3.488(1)	3.481(1) [3.479(1)]	3.460(1) [3.457(1)]	3.485(1)	3.491(1) [3.448(1)]	3.472(1)	3.483(1)	3.461(1)	3.487(1)
Ni(1)−S(1)−Ni(2)	90.30(2)	89.89(3)	89.05(5)	88.62(7) [88.62(7)]	87.83(4) [87.20(4)]	88.04(6)	89.51(4) [88.65(4)]	87.98(5)	88.63(4)	88.35(4)	88.92(3)
Ni(1)−S(2)−Ni(2)	92.01(2)	91.98(3)	90.03(5)	89.28(7) [89.22(7)]	92.07(5) [92.27(4)]	92.50(6)	89.60(4) [88.58(4)]	90.95(4)	90.66(3)	90.82(3)	91.33(2)
Ni−S−Ni	91.15(2)	90.94(3)	89.54(5)	88.95(7) [89.07(7)]	89.95(5) [89.74(4)]	90.27(6)	89.56(4) [88.62(4)]	89.47(5)	89.65(4)	89.59(4)	90.13(3)
Ni(1)−O(1)−C(39)	133.16(14)	133.0(2)	133.3(4)	133.3(4) [134.4(4)]	133.9(3) [135.0(3)]	133.1(4)	133.8(2) [132.9(2)]	133.1(3)	134.8(2)	134.3(2)	132.6(1)
Ni(2)−O(2)−C(39)	131.37(14)	132.6(2)	132.4(3)	133.7(4) [133.8(4)]	134.1(3) [133.0(3)]	133.1(4)	133.0(2) [131.7(2)]	135.0(2)	133.3(2)	134.3(2)	135.7(1)
C(4)···C(20)	9.138(2)	9.674(2)	8.825(6)	8.564 [8.690]	9.489 [9.563]	9.589	8.693 [8.948]	9.327	9.306	9.306	9.532
Ph/Ph[c]	76.9	89.6	70.0	63.8 [66.7]	86.4 [87.8]	92.0	67.4 [72.5]	81.3	80.8	81.8	86.5
M^1L_4/M^2L_4	135.2	134.8	134.9	134.7 [134.5]	135.2 [135.3]	135.1	134.7 [134.9]	134.6	134.9	136.1	135.5

[a] There are two crystallographically independent molecules A and B in the unit cell. Values in square brackets refer to the corresponding bond lengths of molecule B. The numbering of the atoms was carried out in such a fashion that Ni1−S1 > Ni1−S2 and Ni2−N6 > Ni1−N1. [b] Average values. [c] Angle between the normals of the planes of the two aryl rings of L^{2-}.

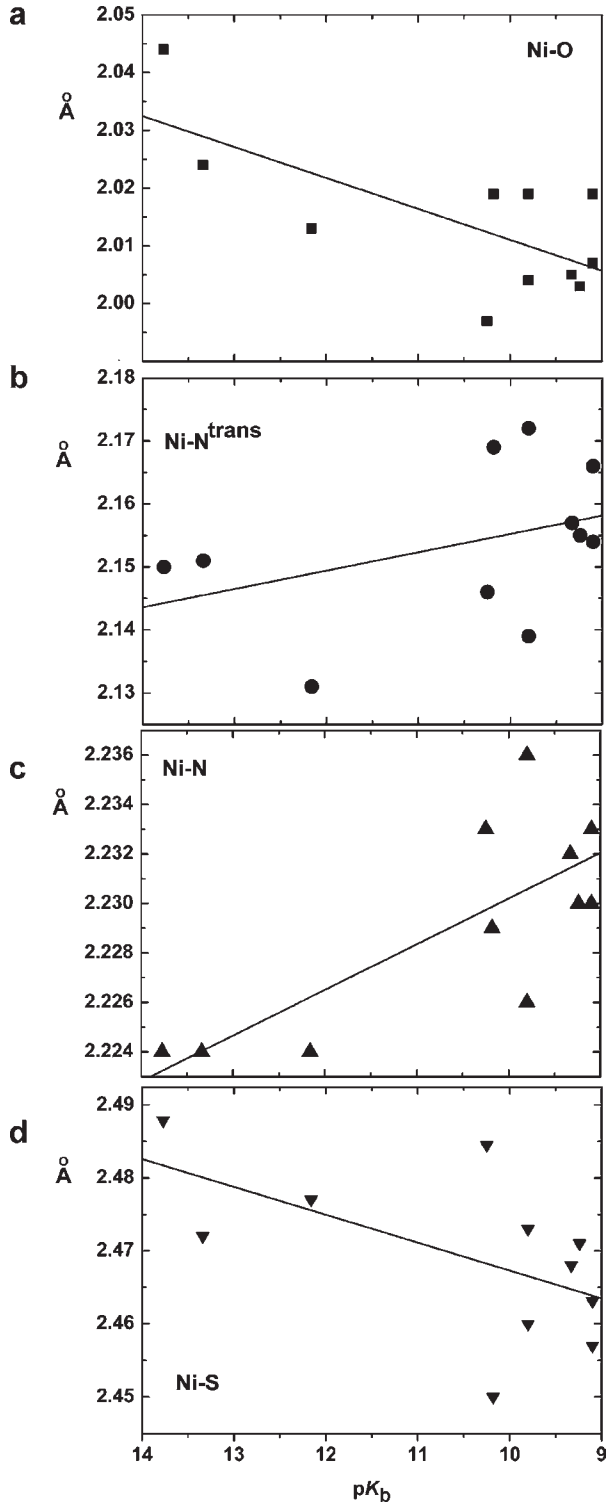

Figure 7. (a−d) Plot of average Ni−O (a), Ni−N^{trans} (b), Ni−N (c), and Ni−S (d) bond lengths in the $[Ni^{II}_2L(\mu\text{-}O_2CR)]^+$ complexes (**2**, **3**, **5**, **8**−**11**, **15**, **17**, **19**, **20**) versus the pK_b value of the carboxylate coligand. The solid lines represent the best linear fits (correlation coefficients: (a) 0.703, (b) −0.403, (c) −0.757, (d) 0.570).[79]

This may be attributed to the fact that the CH···π interactions operate perpendicularly to the Ni−O bonding interactions, as indicated in Figure 5. Hence, the CH···π interactions do not reinforce the Ni−O bonds and do not contribute to the crystal field splitting parameter Δ_o.

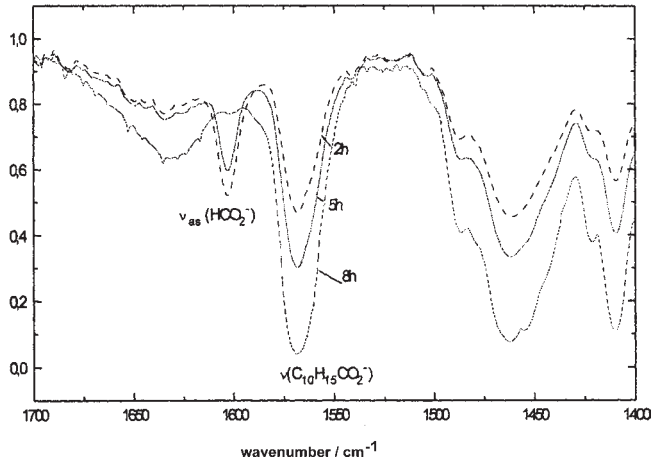

Figure 8. IR spectra of the crude product obtained after workup of the reaction between **8** and sodium adamantate in MeOH/MeCN at 50 °C after 2 h, 5 h, and 8 h (1700−1400 cm^{-1} region).

Description of the Crystal Structures. Previously, only $[Ni^{II}_2L(\mu\text{-}O_2CR)]^+$ complexes with relatively basic carboxylato coligands (i.e., pK_b = 9−10) have been crystallographically characterized. To correlate Ni−O bond distances with the pK_b values it was necessary to examine the structures of further $[Ni^{II}_2L(\mu\text{-}O_2CR)]^+$ complexes. In this study, the crystal structures of compounds **2**, **3**, and **5**, bearing the weakly basic trifluoroacetate, trichloroacetate, and propiolate ($HC{\equiv}C{-}CO_2^-$) ions, respectively, have been determined. The structure of the adamantate complex **19** was also studied to evaluate if the Ni−O bond lengths depend on steric effects. Table 3 lists the data collection and processing parameters for the four new structures. ORTEP views of the structures are presented in Figure 6, and selected bond lengths and angles are given in Table 4. The metrical data for the known structures of **8**−**11**, **15**, **17**, **19**, and **20** are included in Table 4 for comparison. The atom numbering scheme used for the central $N_3Ni(\mu\text{-}SR)_2(\mu\text{-}O_2CR)NiN_3$ core in **2** was applied for all complexes to facilitate structural comparisons.

All complexes are composed of well-separated $[Ni^{II}_2L(\mu\text{-}O_2CR)]^+$ cations, BPh_4^- anions, and MeCN or EtOH solvate molecules. In each case, the macrocycle assumes a "bowl-shaped", calixarene-like conformation generating a $(fac\text{-}N_3)Ni^{II}(\mu\text{-}SR)_2(\mu_{1,3}\text{-}O_2CR)Ni^{II}(fac\text{-}N_3)$ core, as observed in all previously reported $[Ni^{II}_2L(\mu\text{-}O_2CR)]^+$ structures.[8,14] The complexes are essentially isostructural and the corresponding bond lengths and angles lie within very narrow ranges.

Figure 7 represents plots of the average Ni−O, Ni−N^{trans} (Ni−N2 and Ni−N5), Ni−N, and Ni−S bond lengths against the pK_b value of the corresponding free carboxylate ion. The solid lines represent the best linear fits. The correlation coefficients of 0.703, −0.403, −0.757, and 0.570, respectively, are indicative of only poor correlations, but the trends are obvious.[79] Thus, as can be seen, the Ni−O distances decrease steadily with increasing carboxylate basicity, from 2.044(3) Å in **2** bearing the

(79) Parameters resultant from linear least-squares fits: (a) d(Ni−O)/[Å] = 1.96(2) + 0.005(2) × pK_b, R = 0.703; (b) d(Ni−N_{trans})/[Å] = 2.18(2) − 0.003(2) × pK_b, R = −0.403; (c) d(Ni−N)/[Å] = 2.249(6) − 0.0018(5) × pK_b, R = −0.757; (d) d(Ni−S)/[Å] = 2.43(2) − 0.004(2) × pK_b, R = 0.57.

Table 5. Carboxylate Exchange Reactions of Various $[Ni^{II}_2L(\mu\text{-}O_2CR)]^+$ Complexes[a,b]

entry	R	R′	solvent	T	time	$[Ni_2L(\mu\text{-}O_2CR')]^+/[Ni_2L(\mu\text{-}O_2CR)]^+$[c]
1	H	$C_{10}H_{15}$	MeOH/MeCN	25 °C	24 h	ca. 80:20
2	H	$C_{10}H_{15}$	MeOH/MeCN	50 °C	8 h	ca. 95:5
3	H	$C_{10}H_{15}$	MeOH	50 °C	6 h	ca. 95:5
4	H	$C_{10}H_{15}$	MeCN	50 °C	4 d	ca. 50:50
5	H	CH_3	MeOH/MeCN	50 °C	8 h	ca. 95:5
6	H	CCl_3	MeOH/MeCN	50 °C	8 h	ca. 95:5
7	Ph	$C_{10}H_{15}$	MeOH/MeCN	50 °C	8 h	no reaction
8	Ph	CH_3	MeOH/MeCN	50 °C	8 h	no reaction
9	Ph	CCl_3	MeOH/MeCN	50 °C	8 h	no reaction

[a] The data refer to the perchlorato complexes. [b] The carboxylates were either supplied as sodium (in MeOH or 50:50 MeOH/MeCN) or triethylammonium salts (in MeCN). [c] The $[Ni^{II}_2L(\mu\text{-}O_2CR')][ClO_4]/[Ni^{II}_2L(\mu\text{-}O_2CR)][ClO_4]$ ratio was determined by visual integration of the ν_{as}(CO) bands in the IR spectrum of the crude product after workup.

weakly basic trifluoroacetate ion to 2.003(2) Å in **17** with the much more basic acetate ion [d(Ni−O)/d(pK_b) = −0.005(2) Å]. The decrease in the Ni−O bonds is coupled with Ni−N and Ni−S bond length changes. Thus, the average Ni−N (or Ni−N^{trans}) distances increase and the Ni−S bond length decreases with increasing basicity of the carboxylate. The average Ni−N and Ni−S bond length changes (per pK_b unit) are smaller than variation of the Ni−O distances (ca. 0.002−0.004 Å), but add up to a significant value of about 0.04 Å over the full pK_b range. There is also a clear correlation between the Ni−S−Ni bond angle and the pK_b value (not shown in Figure 7). With increasing pK_b value, the Ni−S−Ni angle steadily contracts from 91.15(2)° in **2** (trifluoroacetate) to 89.59(4)° in **19** (adamantate). This in turn leads to a decrease of the Ni···Ni distance by about 0.10 Å. All of these trends are also seen for complexes coligated by sterically demanding carboxylate ions (i.e., **10**, **19,** and **20**). This observation excludes the possibility of bond length changes due to steric effects. Overall, the observed correlation between pK_b value and Ni−N and Ni−S bond distances is significant and in good agreement with the conclusions drawn from the UV/vis spectroscopic investigations. The UV/vis spectroscopic differences of the carboxylate complexes are directly related to the bonding features of the carboxylate coligands.

Carboxylate Exchange Reactions. Using IR spectroscopy it has also been possible to study carboxylate exchange reactions. Note that these reactions are less readily investigated by other methods. To probe whether the complexes undergo substitution reactions, two selected complexes, namely, the formato and the benzoato species **8** and **11**, were allowed to react with three different carboxylate ions (adamantate, acetate, trichloroacetate) according to eq 3.[80] Samples (5 mL) of the reaction mixtures were removed at regular intervals, an excess of $LiClO_4$ was added, and the solution concentrated to about 2 mL to precipitate the reaction product and unreacted starting material. The solid was then filtered, dried and analyzed by IR spectroscopy. The relative amounts of starting materials and products were estimated from the relative intensities of the corresponding ν_{as}(CO) bands.[81] A typical set of spectra is presented in Figure 8. The reaction data are presented in Table 5. Given the uncertainty of the visual integration method used these data should be taken as indicative rather than definitive.

The most important results of these studies are as follows: (*i*) The $[Ni^{II}_2L(\mu\text{-}O_2CR)][ClO_4]$ complexes are relatively inert to substitution reactions. As can be seen from entries 1−4, the best reaction conditions include the polar, protic solvent MeOH, an excess of the sodium carboxylate and elevated temperatures 50 °C. Even under these optimized conditions, about 8 h are required to drive the respective substitution reactions to completion (entries 1−6). (*ii*) Of the two complexes investigated exemplarily, only the formato-bridged complex **8** underwent substitution reactions (entries 1−6), whereas no reaction was observed with the benzoato complex (entries 7−9). (*iii*) The formato coligand could be replaced by both more and less basic carboxylate ions (entries 5 and 6).

$$[Ni^{II}_2L(\mu\text{-}O_2CR)][ClO_4] + R'CO_2^- \rightarrow [Ni^{II}_2L(\mu\text{-}O_2CR')][ClO_4] + RCO_2^- \quad (3)$$

The observations made for the formato complex **8** can be rationalized by taking into account the UV/vis spectroscopic results described above showing only small stability differences of the various carboxylato complexes[76] and the thermodynamic control of the equilibrium described in eq 3. If, to a first approximation, the relative stabilities $K_{rel} = \exp(\Delta\Delta G/RT)$ of a pair of two complexes is related to the difference in LFSE (i.e., $\Delta\Delta G = \Delta_{LFSE}$), one can calculate equilibrium constants of K_{rel} = 3.44, 0.65, and 0.28 for the exchange reactions of **8** with trichloroacetate, acetate, and adamantate ($C_{10}H_{15}CO_2^-$), respectively.[82] It can easily be shown for all three equilibria that the reaction conditions employed (i.e., 10-fold molar excess of the carboxylate ions) are sufficient to drive the reaction to near completion, as also established by IR spectroscopy.[83]

The observations made for the benzoato complex are unexpected. If one uses the same arguments as above,

(80) The sodium or triethylammonium carboxylates were added in a 10-fold molar excess. At lower molar ratios, the reactions were too slow and inconvenient to study.

(81) All complexes have very similar solubility properties. It is therefore very unlikely, that the equilibrium in eq 3 is influenced by solubility differences.

(82) $\Delta\Delta G(\mathbf{3},\mathbf{8}) \cong \Delta_{LFSE(\mathbf{3},\mathbf{8})} = 1.2 \times [\Delta_o(\mathbf{3}) - \Delta_o(\mathbf{8})] = 1.2 \times 214\ cm^{-1} \times 11.96\ J/(mol\ cm^{-1}) = 3.06\ kJ/mol$; $\Delta\Delta G(\mathbf{17},\mathbf{8}) = 1.2 \times (-112\ cm^{-1}) \times 11.96\ J/(mol\ cm^{-1}) = -1.61\ kJ/mol$; $\Delta\Delta G(\mathbf{20},\mathbf{8}) = 1.2 \times (-48\ cm^{-1}) \times 11.96\ J/(mol\ cm^{-1}) = -0.688\ kJ/mol$; $K_{rel} = \exp(\Delta\Delta G/(RT))$.

(83) $x = [HCO_2^-]$, [**3**], [**19**], or [**20**]; $K_{rel} = [x][x]/[c_0-x][10c_o-x]$. For c_0 = 0.001, $x \sim 0.00097$, 0.00087, and 0.00077 (corresponding to 97%, 87%, and 77% conversions).

exchange reactions of complex **11** should be thermodynamically feasible in all cases as well. The observed "inertness" is most likely due to kinetic factors such as steric hindrance, which slow down the reactions, or to secondary interactions (and hence unfavorable low equilibrium constants) or both. The truth must await further kinetic studies, which are the focus of current investigations.

Concluding Remarks

The main findings of the present work can be summarized as follows: (*i*) The macrocycle L^{2-} allows preparation and isolation of a series of isostructural $[Ni^{II}_2L(\mu\text{-}O_2CR)]^+$ complexes with different carboxylate pK_b values ($pK_b = 9-14$). (*ii*) The $[Ni^{II}_2L(\mu\text{-}Cl)]^+$ complex **1** reacts readily with sodium or triethylammonium carboxylates and represents a versatile starting material for the $[Ni^{II}_2L(\mu\text{-}O_2CR)]^+$ species. Substitution reactions are not affected by varying basicity or steric hindrance of the entering carboxylate groups. (*iii*) In contrast to the corresponding $[Zn^{II}_2L(\mu\text{-}O_2CR)]^+$ complexes which typically exchange their carboxylates on the NMR time scale,[8] the $[Ni^{II}_2L(\mu\text{-}O_2CR)]^+$ complexes are relatively inert to substitution reactions attributable (in part) to the ligand field effects associated with the d^8 electronic configuration of the nickel(II) ($S = 1$) ions. An excess of sodium carboxylate, elevated temperatures of 50 °C, and long reaction times (> 8 h) are required to drive the carboxylate exchange reactions to completion. (*iv*) The formato coligand in **8** can be replaced by both more and less basic carboxylates. The benzoato-bridged complex **11** does not react in any case, a fact attributable to kinetic factors or to the absence (**8**) or presence(**11**) of stabilizing secondary $CH\cdots\pi$ host−guest interactions. (*v*) $[Ni^{II}_2L(\mu\text{-}O_2CR)]^+$ complexes are readily identified by their ν_{as}(CO) and the ν_s(CO) stretching frequencies which lie in the ranges 1684−1576 cm^{-1} and 1428−1348 cm^{-1}, respectively. The scattering can be attributed to the varying basicity of the bridging carboxylato coligand, since their immediate environment in the dinuclear complexes is practically the same. (*vi*) UV/vis spectroscopic examinations reveal that the spin-allowed $^3A_{2g} \rightarrow {}^3T_{2g}$ (ν_1) transition is steadily red-shifted across the series, from 1094 nm in **2** bearing the weakly basic trifluoroacetate ion to 1129 nm in **18** with the much more basic propionate ion. (*vii*) The binding of a basic carboxylato donor affects the macrocycle−nickel(II) interactions. This is reflected in the solid state structures of the complexes by small but significant bond length changes (i.e., the Ni−N bonds shorten and the Ni−S bonds lengthen).

Acknowledgment. We are thankful for Prof. Dr. H. Vahrenkamp and Prof. Dr. H. Krautscheid for providing facilities for spectroscopic and X-ray crystallographic measurements. This work was supported by the Deutsche Forschungsgemeinschaft (Projects KE 585/4-1,2,3), the University of Freiburg and the University of Leipzig. U.L. thanks the graduate school "BuildMona" for a fellowship support.

Supporting Information Available: X-ray crystallographic data in CIF format. This material is available free of charge via the Internet at http://pubs.acs.org.